

# Analysis of Laser Metal-Cut Energy Process Window

Joseph B. Bernstein, Joo-Han Lee, Gang Yang, and Tariq A. Dahmas<sup>1</sup>

**Abstract**—Metal fuses for laser redundant links have been used for years in laser repair application. Nonetheless, there have been reliability problems for laser metal cut structures such as the material leftover remaining at the bottom of the cut-site and/or the formation of lower-corner crack. In this paper, a special finite element Two-Stage Laser Cut Simulation Model (TSLCSM) is proposed to study the cut process. Compared to other simulation methods for similar purposes, the proposed model not only includes the stress-relief effect due to cracking and breakthrough of passivation caused by upper-corner cracks, but also explains the laser-cut mechanism ignoring of metal underlayer. It proves earlier experimental results that a laser energy window exists for each cut structure under a specified laser pulse. Different laser cut structures and different laser parameters are considered in the simulation and useful guidelines are obtained for maximum laser energy process window. Experimental observations consistent with simulation results show that the differential between upper-corner stress and lower-corner stress is temporarily dependent on the passivation breakthrough caused by upper-corner cracks. Also, it is shown that lower-corner cracks can be formed at much lower laser energies than previously expected.

**Keywords**—Laser processing, laser metal cut, process window, stress-relief, fuse, yield enhancement.

## I. INTRODUCTION

LASER technologies have been used to process microelectronic devices for more than two decades. This technology has found the greatest application in devices which exhibit large-scale redundancy in their designs [1]. A laser is employed to remove defective elements and replace them with redundant ones.

In order to achieve successful laser-cutting of metal lines, material leftover at the bottom of cut-site and lower-corner cracks have become a major reliability issue. These two failure phenomena prevent the line from being completely disconnected and cause substrate damage as well [2], [3]. Laser processing involves the action of complex thermal and mechanical coupled mechanisms within a very short time frame of laser impingement. Therefore, it is essential to understand the kinetics in order to improve the reliability of laser processing.

Computer simulation models have been used to help understand the physical and thermal interactions induced by the laser within the metal structure. From the analyses of the simulations, proposals for improved cut structures, with better performance, have been presented [4], [5], [6]. In this work, an analysis of the developments of upper and

lower-corner cracks produced by the laser cutting of aluminum lines is presented. The results of computer simulations as well as experimental observations are both detailed in order to better understand the metal cutting process. The concept of a “process window” for reliable line cutting is also presented.

## II. DYNAMICS OF CRACK FORMATION

Laser-induced line cutting is achieved by the complex interplay of both mechanical and thermal mechanisms. The thermal expansion of aluminum, caused by the transfer of energy from a laser pulse, induces the necessary mechanical mechanisms. Eventually, the mechanical action displaces the metal from the line. Together, these mechanisms combine to remove the intended material from the wafer surface.

The removal of metallic material is initiated by the application of a laser pulse to the designated cut-site of the aluminum line. Since the silicon nitride and silicon dioxide passivation layers are “transparent” to the laser spectrum (as compared to aluminum), most of the laser energy is absorbed by the metal line. Once the aluminum (or more accurately the metal over-coating) absorbs this energy, the temperature of the metal line increases. An increase in the temperature causes the metal to expand and, in turn, induces high tensile stress around the metal line in the surrounding dielectric layers.

The amount of stress generated around the metal line is mainly dependent upon the metallization geometry and the degree of mismatch between the thermal expansion coefficients of aluminum and the silicon dioxide surrounding it. Rectangular shaped cross-section of metallization causes high tensile stresses to be focused on the both upper and lower-corners of the metal line where laser pulse hits. Since the dielectric layer (silicon dioxide) is thicker below the line than above, greater stress will be induced at the upper-corners of the metal line, even when assuming a uniform temperature profile across aluminum line [7]. When accounting for a non-uniform temperature profile, due to the limited absorption depth of the initial stages of the laser pulse, the difference in stress between the upper and lower-corners will be even greater. The thermal profile within an aluminum line, over a period of a laser pulse, was presented by R. Rasera *et al.* [8].

Once a critical stress,  $\sigma_c$ , is reached, a crack is initiated at each of the upper-corners. Initiating from the upper-corners, the cracks tend to move perpendicularly to the local maximum principal tensile stress. Due to the brittle behavior of the glassy passivation, this crack propagates

Authors are with Department of Materials and Nuclear Engineering, University of Maryland at College Park, 2100 Marie Mount Hall, College Park, MD 20742-7531, phone: (301)405-5038, fax: (301)314-9437, E-mail: jooohan@glue.umd.edu. <sup>1</sup>Tariq A. Dahmas is currently with IBM Microelectronics Division, Essex Junction, VT 05452 phone: (802) 769-9946 e-mail: tariqd@us.ibm.com.

through the dielectric layers to the surface. It is considered that a crack initiates before superheated Al melts due to the hard surrounding passivation. The propagation of the cracks to the surface allows the metal to melt due to the pressure release caused by cracking and creates an explosion which ejects the metal away from the cut-site. Further studies are being continued to simulate the material yielding and the initiation and propagation of the cracks.

If the entire cross-section of aluminum melts (due to the diffusion of heat from the surface) when the passivation layer is ejected, then the molten aluminum will be removed at the instant that the explosion occurs. Simulations of crack formation (for rectangular line geometry) reveal that cracking at the lower-corners will also occur at high energies, but only after upper-corner cracking occurs.

It has been observed from experiments that the laser metal cut process is dependent upon the energy of the laser pulse used [2]. If the laser energy is too low, then some metal will remain at the bottom of cut-site after the explosion. Therefore, a connection will remain at the cut-site. On the other hand, if the laser energy is too high, then the lower-corners may crack before the explosion occurs. When this happens, molten metal fills the lower-corner cracks. These lower-corner cracks may damage the underlying circuitry and/or result in an incomplete cut [2].

### III. SIMULATIONS

#### A. Two-Stage Laser Cut Simulation Model

To simulate the crack formation process, a custom Finite Element Model (FEM) was utilized. The model, known as the Two-Stage Laser Cut Simulation Model (TSLCSM), was simulated using the MARC *Mentat II* software. The stress evolution at the upper and lower-corners was determined by dividing the model into two distinct stages, Stage 1 and Stage 2. These are illustrated schematically in Fig. 1, but you can refer to the cross-sectional images of Fig. 4 - 6 to see the correspondence with this representation.

The Stage 1 model, Fig. 1(a), depicts the situation during the initial period of laser heating, prior to crack initiation at the upper-corner. This stage of the model covers the period of time between the application of the laser pulse and the initiation of a crack at the upper-corner. After the crack is generated, a transition period occurs in which the stress at the lower-corner begins to release. Propagation of the crack to the free surface occurs during this transition period. The transition period concludes when the passivation breaks. The Stage 2 model, Fig. 1(b), covers the period of time after the passivation break.

In the TSLCSM simulations, only half of the metal line structure was considered. This was done since the metal line possesses a symmetrical cross-section. We assumed that the anti-reflective overcoating layer of the aluminum and dielectric layer accounted for 50% absorption of the impinging laser energy. Overcoating and undercoating layer were not considered in the mechanical simulation. The symmetric (vertical) axis of the simulation model was assumed to only exhibit vertical displacement. The other vertical axis (depicted on the right side of Fig. 1(a)), as

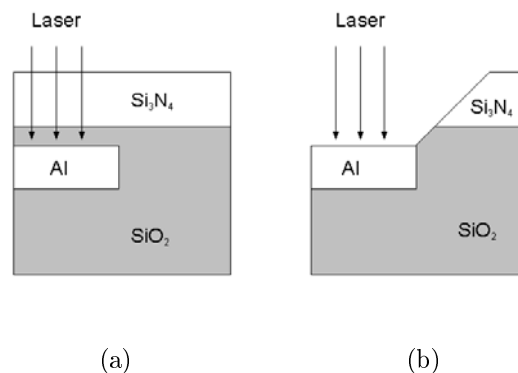


Fig. 1. Two-Stage Laser Cut Simulation Model(not drawn to scale). (a) Stage 1 and (b) Stage 2.

well as the bottom horizontal axis were treated as boundaries where no displacements and no temperature changes could occur.

The laser pulse was simulated to impinge on the surface of the wafer in the manner depicted in Fig. 1(a). In addition, heating by the laser was simulated by heat flux from the top of the metal, obeying a Gaussian distribution [9]. Heating of the metal structure was considered only along its cross-section.

Since most of our concerns are at the upper and lower-corners of the metal structure, a mixed quadrilateral-triangle mesh was used for the simulations. This was done in order to make sure that there were enough elements around the corners of the structure. It has been proven that the results obtained from this mesh scheme are comparable with the traditional all-quadrilateral scheme [10]. The computation time was also largely decreased due to the fewer mesh elements.

#### B. Results of Simulations

##### B.1 Simulation Curves

Sample simulation curves of the induced stress, at the upper and lower-corners of metal line under the laser heating, as a function of time is illustrated in Fig. 2. The induced stresses are plotted on the vertical axis, in units of GPa and time is plotted on the horizontal axis, in units of ns. The three curves that are plotted are actually the results of both simulation stages, Stage 1 and Stage 2, merged together. Stage 1 begins at time 0 and ends at time  $t_1$  (the initiation of the upper-corner crack), while Stage 2 begins at time  $t_2$  (passivation break). The curve for the stress at the upper-corner, however, is only depicted for Stage 1 (labeled *Upper-corner*).

The simulation results reveal that both the upper-corner stress (*Upper-corner*) and the lower-corner stress (*Lower-corner(Stage 1)*) begin to develop immediately when the laser pulse impinges on the structure. However, the stress at the upper-corner is greater than that at the lower-corner. This result is consistent with results of earlier works [7], [8]. The critical stress (stress necessary for crack initiation) at the upper corner,  $\sigma_c$ , occurs at time  $t_1$  in Fig. 2 where

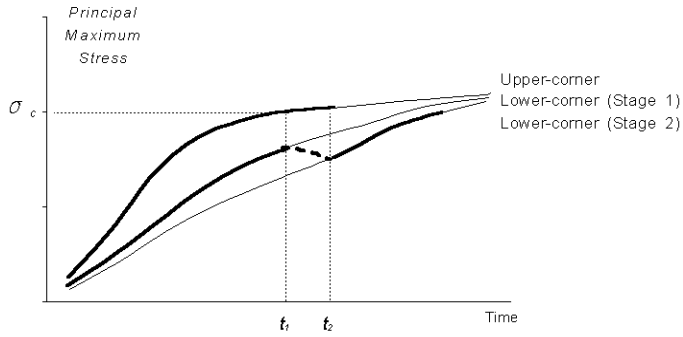


Fig. 2. Result: Sample curve of Two-Stage Laser Cut Simulation.

the crack is assumed to initiate at upper-corner. In the simulations, it was assumed that the stress at the upper-corner continued to develop along the same curve, even after the development of a crack and follow the same curve until the time  $t_2$  when the crack reaches the free surface. It is certain that the upper-corner stress would disappear after  $t_2$ .

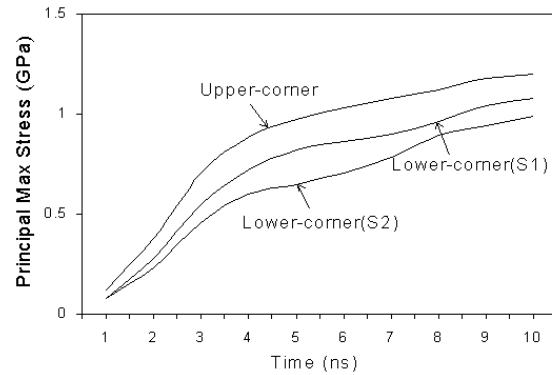
The release of stress at the lower-corner, as a result of crack development at the upper-corner, is indicated by the dashed curve in Fig. 2 connecting *Lower-corner(Stage 1)* and *Lower-corner(Stage 2)*. When the upper-corner crack breaks the overlying passivation, at time  $t_2$ , it is assumed that the lower-corner stress begins to follow *Lower-corner(Stage 2)*. At this moment, the Stage 2 model in Fig. 1(b) is employed to simulate the stress-relief effect. The end of the simulations occurs when the controlled explosion takes place and material is ejected from the cut-site.

It is noticed that the stress at lower-corner will be reduced again after a laser pulse as the metal line cools down; however, the curves in Fig. 2 shows the duration of a laser pulse and we do not consider the stress release after the laser pulse.

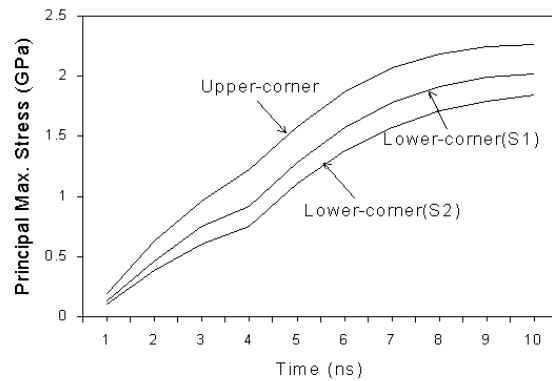
## B.2 Laser Cut Process Cases

TSLCSM simulations using different laser energies were performed to illustrate the three main outcomes for a laser cut process. In these simulations, an aluminum line measuring  $0.4\mu\text{m}$  thick and  $2.0\mu\text{m}$  wide, with a  $1.0\mu\text{m}$  passivation layer, was used. A  $15\text{ns}$  triangular laser pulse, with a peak at  $3.25\text{ns}$  and a round  $1/e^2$  spot size of  $4.25\mu\text{m}$  in diameter, was utilized to simulate the cut process. Laser energies of  $0.3\mu\text{J}$ ,  $0.5\mu\text{J}$ , and  $1.2\mu\text{J}$ , were selected for these simulations. Prior to the impingement of the laser, the structure was assumed to be at room temperature with zero tensile stress.

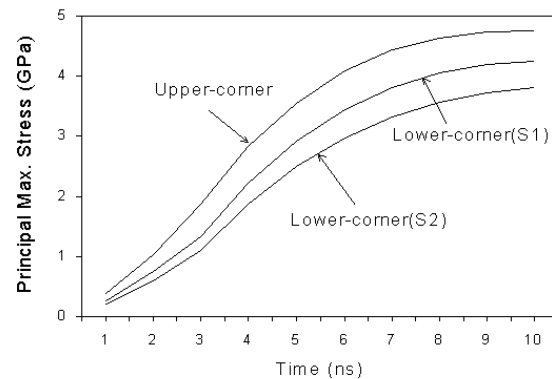
In each of the three simulations, the upper-corner critical stress was assumed to be  $1\text{GPa}$  [11]. The crack propagation speed was considered to be dependent on the laser energy. That is, a higher laser energy produced a higher propagation velocity. However, for simplicity, the time for crack propagation was assumed to be  $1\text{ns}$  throughout the



(a)



(b)



(c)

Fig. 3. Results of Two-Stage Laser Cut Simulation with various laser energies, spot size:  $4.25\mu\text{m}$   $1/e^2$  diameter. Laser energies: (a)  $0.3\mu\text{J}$ , (b)  $0.5\mu\text{J}$ , and (c)  $1.2\mu\text{J}$  [10].

simulations. This assumption was based on the fact that the crack propagation speed is limited to approximately 1/3 the speed of sound in the brittle, solid materials [12]. Therefore, a time of 1ns is needed for the crack to propagate through a  $1\mu\text{m}$  thick passivation layer. Additionally, for simplicity, the explosion and ejection of material were assumed to occur at the same time that the crack penetrated the free surface (i.e. at time  $t_2$ ), even though the explosion happens after passivation breakthrough.

The results of the simulation of a  $0.3\mu\text{J}$  laser energy are displayed in Fig. 3(a). As seen in the graph, an upper-corner crack was initiated at time  $t_1 = 5.5\text{ns}$ . Therefore, at time  $t_2 = t_1 + 1 = 6.5\text{ns}$ , the crack reaches the free surface and the ejection of material occurs.

The time for complete melting of the metal structure was calculated (by the simulation program) to occur at 8.8ns. Therefore, from the simulation for a  $0.3\mu\text{J}$  laser energy, at time  $t_2$  the heat diffusion from the surface did not melt the entire metal structure. As mentioned above, this incomplete melting causes some aluminum to remain at the bottom of the cut-site after the ejection of material.

When the laser energy was increased to  $0.5\mu\text{J}$ , initiation of the upper-corner crack was simulated to begin at time  $t_1 = 3.2\text{ns}$ . The simulation results are displayed in Fig. 3(b). In this case, the diffusion of heat in the aluminum line caused the aluminum to completely melt at the same time that the crack penetrated to the free surface ( $t_2 = 4.2\text{ns}$ ). Therefore, all the molten aluminum, as well as the passivation layer of the cut-site, was ejected by the cut process.

When a laser energy of  $1.2\mu\text{J}$  was applied, initiation of the upper-corner crack was simulated to occur at time  $t_1 = 2.0\text{ns}$ . The simulation results for this case are displayed in Fig. 3(c). For this case, however, the diffusion of heat in the metal structure caused the entire structure to melt (at time  $t = 2.9\text{ns}$ ) before the crack reached the free surface (at time  $t_2 = 3.0\text{ns}$ ). Also the lower-corner stress (*Lower-corner(S2)*) reached  $\sigma_c$  before  $t_2$ . This results in the development of a lower-corner crack.

From the results of the three cases, it is apparent that the stress difference between the upper and lower-corners (for the same instant of time) increases when the laser energy is increased. However, a higher energy also increases the lower-corner stress curve (*Lower-corner(S2)*). A steeper slope for *Lower-corner(S2)* indicates that the lower-corner stress achieves the critical value faster. Therefore, the chance that lower-corner cracks will develop is increased.

### B.3 Laser Cut Process Window

The “process window” is a figure of merit used to describe the optimum range of laser energies for cutting metal lines. A lower-bound for reliable processing is given by the minimum energy needed to perform a cut without leaving any remaining metal at the cut-site. An upper-bound for reliable laser processing is given by the maximum energy which can perform a cut without creating a lower-corner crack [2]. The process window is thereby determined by taking the ratio of the upper-bound energy over the lower-

bound energy.

The simulation results indicate that the laser energy, used for cutting, must fall within a specific range, or process window. The wider the process window is, the higher the possibility that a reliable cut will be performed. The range of the process window depends on many factors such as the metal line width, thickness, and passivation thickness, as well as on the parameters of the laser pulse. These variables and the consequent results of various process windows will be addressed in a later section of this paper.

## IV. EXPERIMENTAL

### A. Process Parameters and Test Setup

The test wafer, with the aluminum lines, was fabricated using a standard 2-level metal CMOS process. The upper-level metallization (the metallization used for this study) was sputtered  $Al(1\%Si, 0.5\%Cu)$  etched to form  $1.2\mu\text{m}$  wide and  $0.75\mu\text{m}$  thick lines. A passivation layer, consisting of  $0.7\mu\text{m}$  of  $Si_3N_4$  over  $0.3\mu\text{m}$  of  $SiO_2$ , covered the metallization. The  $Al$  lines were undercoated and overcoated with a  $0.09\mu\text{m}$  thick layer and a  $0.05\mu\text{m}$  thick layer of  $TiN$  respectively.

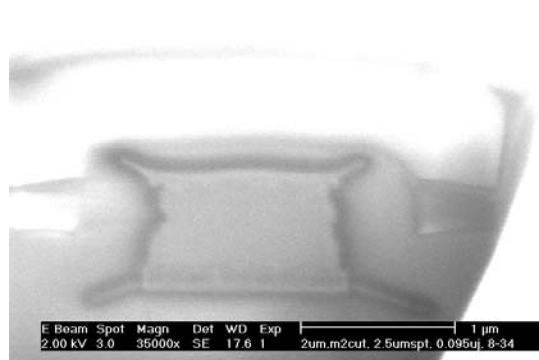
The laser system used to perform the cuts was an *XRL 525* laser process system. The system employs a *Spectra Physics* diode-pumped, Q-switched, Nd:YLF laser ( $1047\text{nm}$ ) operated in the saturated single-pulse mode. Pulses, with lengths of approximately 15ns, were directed through focusing optics to produce a beam  $1/e^2$  diameter of approximately  $4.25\mu\text{m}$  (at focus). The positioning accuracy of the laser system was approximately  $0.5\mu\text{m}$ . For the experiments, a series of laser energies, between  $0.05\mu\text{J}$  and  $1.535\mu\text{J}$  (in steps of  $0.015\mu\text{J}$ ) were used.

Electrical measurements of processed cuts revealed unreliable data due primarily to the difficulty in completing the removal of the TiN barrier layer. Thus, we concentrated on studying the phenomenon of lower-corner cracking through FIB analysis since it was able to yield more consistent results that could be modeled by our FEA software. Of course we can not ignore the subsequent removal of the lower barrier material. Other considerations that were not addressed in this study include laser offset and the optical interference effects due to the thicknesses of the passivation layers.

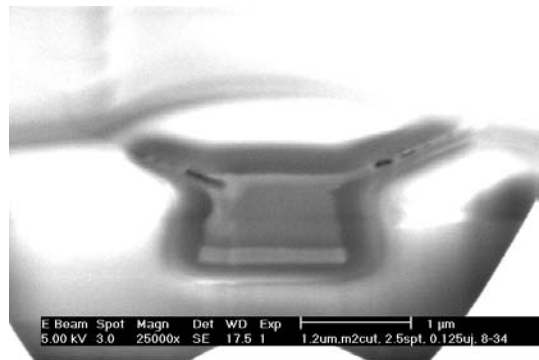
Analysis of the laser cut processing was performed using a *Dual Beam 620D* focused ion beam (FIB) and scanning electron microscope (SEM) system manufactured by FEI. The system was used to obtain cross-sectional images of the processed cut-sites and to investigate the crack evolution at the upper and lower-corners. The FIB cross-sections were made perpendicular to the wafer surface and parallel to the direction of the laser beam.

### B. Experimental Observations

Fig. 4(a) displays the cross-sectional view of a cut-site processed with a laser energy lower than the threshold energy needed for the aluminum to break through the passivation. The image clearly reveals that the laser energy was



(a)



(b)

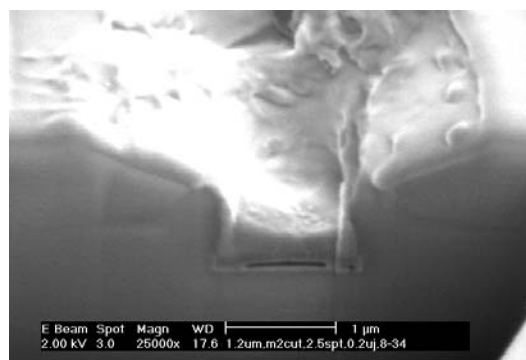
Fig. 4. FIB cross-sectional images of laser-cut sites processed with energies below the process window, spot size:  $4.25\mu\text{m}$   $1/e^2$  diameter. Laser energies: (a)  $0.095\mu\text{J}$  and (b)  $0.125\mu\text{J}$ .

not high enough to perform the cut operation. The passivation layer was not removed by an explosion, therefore the metal could not be ejected from the cut-site.

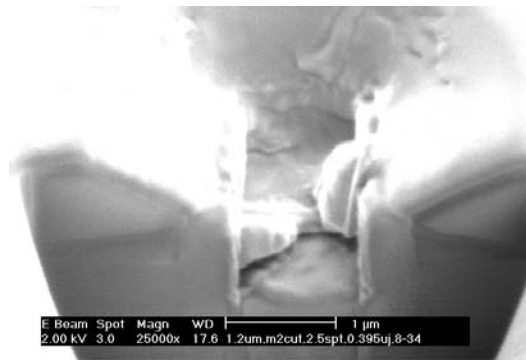
In the case of Fig. 4(a), a laser energy of  $0.095\mu\text{J}$  was used. Instead of the ejection of material, Al-filled lower-corner cracks were generated by the failed cut-process. Although upper-corner cracks were initiated, the stress-relief effect caused by them was not enough to prevent the lower-corner stress from generating cracks. The Al-filled, lower-corner cracks in Fig. 4(a) also indicate that the heat diffusion, generated by the laser energy, was able to melt the Al metal all the way down to the bottom of the structure. This melting, without the occurrence of an explosion, was achieved even at a low laser energy.

The physical characteristics of the cracks provide hints about the development of stress over time in the metal structure. Due to imperfect processing, the metal line did not possess a rectangular cross-section. Instead, the cross-section was trapezoidal, with upper-corners of obtuse angles. This geometry seems to have resulted in the development of greater stress at the lower-corners. Consequently, lower-corner cracking was initiated at the same energy as upper-corner cracking.

The low energy development of lower-corner cracks may have been caused by the presence of the hard silicon nitride overcoating of the metal structure. Silicon nitride, which is harder than the silicon dioxide, seems to have retarded



(a)



(b)

Fig. 5. FIB cross-sectional images of laser-cut sites processed with energies between the passivation-break threshold energy and the upper-bound of process window, spot size:  $4.25\mu\text{m}$   $1/e^2$  diameter. Laser energies: (a)  $0.2\mu\text{J}$  and (b)  $0.395\mu\text{J}$ .

the propagation of the upper-corner cracks. Therefore, the stress at lower-corners of the structure prevailed in the process.

Fig. 4(b) shows a cross-sectional view of a cut-site processed using a laser energy higher than threshold energy necessary to break the passivation completely (passivation-break threshold energy). In this case, a laser energy of  $0.125\mu\text{J}$  was used. Although the passivation was broken, the laser energy was still below the lower-bound needed to process reliable cuts.

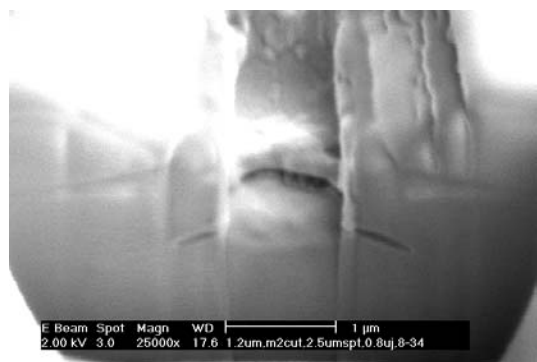
The figure shows the successful break of cracks from both upper corners, through the passivation, to the free surface. Lower-corner cracks, on the other hand, did not develop. This indicates that lower-corner cracks are not as likely to develop as the laser energy is increased above the passivation-break threshold energy. Thus we see that the passivation break by the upper-corner cracks relieves stress from the lower-corners. This stress-relief is large enough to avoid lower-corner cracks.

A higher energy, such as the one used to process the cut-site in Fig. 5(a) ( $0.2\mu\text{J}$ ), produces similar effects to processing with shorter laser pulses. That is, both methods heat up the upper section of the metallization within a very short period of time. Therefore, both methods accelerate the upper-corner cracks.

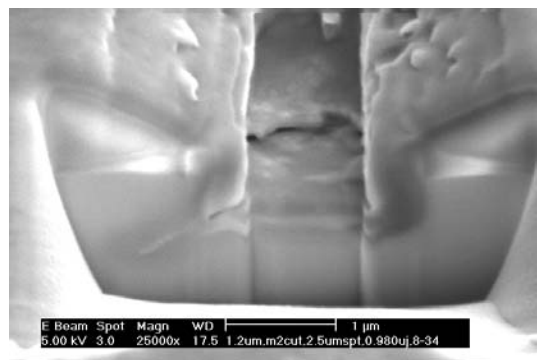
The image reveals that the upper-corner crack was initi-

ated and propagated to the free surface (thereby initiating the explosion) well before the entire metal structure was able to melt. Therefore, metal remained at the bottom of the cut-site. Notice how the  $TiN$  underlayer, in Fig. 5(b), was beginning to peel off at this laser energy.

In the case of Fig. 5(b) a laser energy of  $0.395\mu J$  was used. The cross-sectional image portrays a clean, reliable cut. All of the aluminum, as well as the  $TiN$  undercoating, was removed by the cut process. The absence of lower-corner cracks indicates that the melting of the entire  $Al$  structure and the explosion occurred at approximately the same time. Therefore, the image indicates that the laser energy used was within the process window. However, lower-corner cracks may develop, even if an energy within the process window is used, if errors, such as a positioning offset of the laser spot, are introduced into the cut processing of narrow metal line.



(a)



(b)

Fig. 6. FIB cross-sectional images of laser-cut sites processed with energies above the process window, spot size:  $4.25\mu m$   $1/e^2$  diameter. Laser energies: (a)  $0.8\mu J$  and (b)  $0.98\mu J$ .

The results of using high energy laser pulses to process cuts are displayed in Fig. 6. These figures illustrate the effect of using a laser energy above the process window. In the first case, a laser energy of  $0.8\mu J$  was used. The image reveals unfilled lower-corner cracks which indicate that lower-corner cracking was initiated before the  $Al$  structure fully melted. In this state, the  $Al$  line is considered to be a superheated solid at the time of crack initiation, due to the high pressure induced under the hard passivation. When the pressure is released, in a dramatic manner, the metal

is likely to melt instantly and explode.

The laser energy used to obtain Fig. 6(b) was  $0.980\mu J$ . This energy is far beyond the process window. The image clearly shows the long, undesirable lower-left corner crack. The length of the crack poses a reliability concern, since it may form a short-circuit or damage surrounding structures. The asymmetric cracking is due to the laser-spot positioning offset.

## V. MORE SIMULATIONS RESULTS

Various metal structure designs and laser parameters were simulated to understand their effects on laser process windows. Specifically, the effect of the metal width, metal thickness, passivation thickness, and laser pulse length on the process window were considered.

It has been reported that narrower metal line increases the probability of generating cracks from the lower-corners as well as upper-corners of  $Al$  metal line [7]. Our simulation reveals consistent results with the earlier work. The narrower the metal width, the narrower the energy process window. This is due to the fact that a wider line increases the stress difference between the upper and lower-corners. Therefore, greater laser energy can be adopted for wider metal lines without failure. Unfortunately, this is contrary to the industrial trend of decreasing the fuse pitch by using narrower lines.

Laser cut structures with different metal and passivation thicknesses were also simulated in order to determine how they influence the energy process window. Fig. 7 illustrates the process windows obtained using various combinations of passivation and metal thicknesses. For these simulations, four different passivation thicknesses ( $0.2\mu m$ ,  $0.6\mu m$ ,  $1.0\mu m$ , and  $1.8\mu m$ ) and three different metal thicknesses ( $0.4\mu m$ ,  $0.6\mu m$ , and  $0.8\mu m$ ) were used.

Fig. 7 shows that the maximum possible energy process window obtainable from these combinations is 6:1. This process window occurs when using a  $0.6\mu m$  metal thickness and a  $0.6\mu m$  passivation thickness. From the graph, it is also apparent that it is difficult to obtain an acceptable energy window, even using a  $1.8\mu m$  passivation thickness, when adopting  $0.8\mu m$  metal thickness. We can conclude that an optimal passivation thickness for a specific metal thickness, under a specified laser pulse length, exists. From the simulations, a  $0.6\mu m$  thick passivation is optimal for both  $0.4\mu m$  and  $0.6\mu m$  thick aluminum lines (using a 15ns of laser pulse).

There is also an optimal metal thickness for a specific passivation thickness (under specified pulse length). From Fig. 7, it can be seen that a  $0.6\mu m$  thick aluminum line is optimal for all of the passivation thicknesses that were simulated (using a 15ns laser pulse).

The results of similar simulations with laser pulse of 5ns reveal that the process windows for thin metal line and passivation layer increase. Especially, the process window for  $0.4\mu m$  thick aluminum line with  $0.2\mu m$  passivation layer is prominently increased. The reason for such behavior stems from the fact that the thermal diffusion length in aluminum is proportional to  $\sqrt{t}$ . Equation (1) indicates a

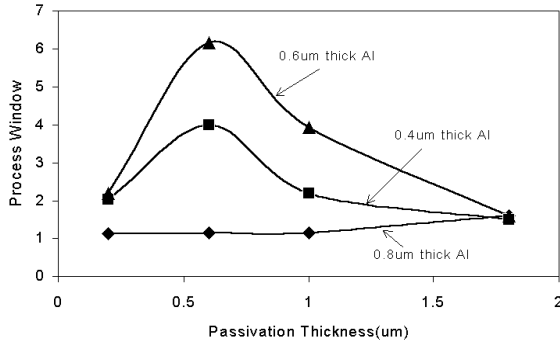


Fig. 7. Laser energy process window with various combinations of passivation and metal thicknesses(laser pulse : 15ns).

simple calculation based on the simulation results to get optimal metal thickness( $T_{metal}$ ) from the pulse length of the laser used( $t_{pulse}$ ).

$$T_{metal} = 0.167\sqrt{t_{pulse}} \quad (1)$$

The calculations show that  $0.65\mu\text{m}$  and  $0.37\mu\text{m}$  of Al line thickness are optimal for 15ns and 5ns laser pulse, respectively. Further studies are being continued to simulate other pulses consistent with more modern laser repair systems.

## VI. DISCUSSION

Experimental observations showed obvious stress-relief at the moment of passivation breakthrough as simulated. Our experimental observations also revealed asymmetric lower-corner cracks in case of narrow metallization( $1.2\mu\text{m}$  wide) after laser pulses through the various laser energies, including even very low energies(lower than passivation-break threshold energy), due to the lack of stress-relief within small aluminum structure. Improved laser positioning accuracy will help avoid asymmetric lower-corner cracks caused by biased stress development. As the metal width increased, no lower-corner crack was found at very low energy levels as well as within process window.

A shorter, or faster rise-time, laser pulse for processing can also be used to avoid this lower-corner cracking. A shorter laser pulse is desirable because it develops a steeper temperature profile within the aluminum [4]. This steeper temperature profile will increase the slope of the upper-corner stress curve(*Upper-corner*) and decrease that of the lower-corner stress curve(*Lower-corner*( $S_2$ )), in Fig. 2, thereby resulting in a larger gap between the two (for the same instant of time). This will cause the upper section of the structure to heat up and expand fast, thereby decreasing the stress for lower-corner cracking and accelerating upper-corner cracking.

Further observations reveal that *Lower-corner*( $S_2$ ) eventually intersects with *Upper-corner* in Fig. 2. This eventual intersection is due to the prevailing heat diffusion within the metal structure. From the simulation curves, it can

been seen that the slope of *Upper-corner* decrease after time  $t_1$ . This is due to the increased heat transfer from top of the metal structure to the bottom. When accounting for heat dissipation along the metal line, it is believed that the slope of *Upper-corner* decreases even faster, thereby reducing the gap between *Upper-corner* and *Lower-corner*( $S_2$ ) sooner than in the 2-dimensional case of Fig 2. A refined model is being simulated to include the 3-dimensional cooling effect and will be presented in a later publication.

## VII. CONCLUSIONS

Two-Stage Laser Cut Simulation Model has been simulated to study the metal-cut process. Experimental observations reveal that lower-corner cracks can be formed at low laser-energy level below passivation-break threshold energy. It is also shown through the observations that the stress-relief effect, due to cracking and breakthrough of passivation caused by upper-corner cracks, exists as predicted by simulations. Laser energy process window for the cut process exists and useful guidelines to get the maximum of the process window were obtained through simulations with various cut structures and laser parameters.

## ACKNOWLEDGMENTS

The authors would like to acknowledge the assistance of Wei Zhang and Gao Zhuo in this project.

## REFERENCES

- [1] R. T. Smith and J. D. Chlipala, "Laser programmable redundancy and yield improvement in a 64k dram," *IEEE J. Solid-State Circuits.*, vol. SC-16, pp. 506-514, Oct. 1981.
- [2] J. B. Bernstein, Y. Hua, and W. Zhang, "Laser energy limitation for buried metal cuts," *IEEE Elect. Dev. Let.*, vol. 19, no. 1, pp. 4-6, 1998.
- [3] Y. Hua, "Mechanism and yield study of laser induced link and cut," M.S. thesis, University of Maryland at College Park, 1997.
- [4] J. D. Chlipala, L. M. Scarfone, and C. Y. Lu, "Computer-simulated explosion of poly-silicide links in laser-programmable redundancy for VLSI memory repair," *IEEE Trans. Elec. Dev.*, vol. 36, no. 11, pp. 2433-2439, 1989.
- [5] S. S. Cohen, P. W. Wyatt, and G. H. Chapman, "Laser-induced melting of thin conduction films: Part I - the adiabatic approximation," *IEEE Trans. Elec. Dev.*, vol. 38, no. 9, pp. 2042-2050, 1991.
- [6] Y. Sun, R. Harris, E. Swenson, and C. Hutchens, "Optimization of memory redundancy laser link processing," *SPIE*, vol. 2636, pp. 152-164, 1995.
- [7] Y. Shen, S. Suresh, and J. B. Bernstein, "Laser linking of metal interconnects: Analysis and design considerations," *IEEE Trans. Elec. Dev.*, vol. 42, no. 3, pp. 402-410, 1996.
- [8] R. Rasera and J. B. Bernstein, "Laser linking of metal interconnect: linking dynamics and failure analysis," *IEEE Tans. Comp. Packag. Manufact. Technol.*, vol. 19A, no. 4, pp. 554-561, 1996.
- [9] R. L. Rasera, "Laser linking of metal interconnect: Process considerations and failure analysis using focused ion beam milling," M.S. thesis, Massachusetts Institute of Technology, 1995.
- [10] G. Yang, "Laser energy window simulation for metal cut structure," M.S. thesis, University of Maryland at College Park, 1999.
- [11] M. Finot, Y. L. Shen, A. Needleman, and S. Suresh, "Micromechanical modeling of reinforcement fracture in particle-reinforced metal-matrix composites," *Metallurgical and Materials Transactions*, vol. 25A, pp. 2403-2420, 1994.
- [12] J. A. Collins, *Failure of materials in mechanical design*, p. 34, John Wiley & Sons, New York, 2nd edition, 1993.